

## Magnetic Sensor Using Second Harmonic Change in Magneto-Impedance Effect

Satoko IIDA, Osamu ISHII and Shiro KAMBE

Graduate School of Engineering, Yamagata University, Jounan, Yonezawa, Yamagata 992-0851, Japan

(Received April 13, 1998; accepted for publication May 27, 1998)

This study reports on a magnetic sensor composed of a Cu wire sandwiched between Co-based amorphous ribbons. The impedance of the Cu wire largely depends on the permeability of the amorphous ribbons and changes with an external field. This phenomenon results in a change in the voltage at the fundamental frequency ( $V_{1st}$ ) and that at the second harmonic frequency ( $V_{2nd}$ ) at both ends of the Cu wire. The maximum  $V_{2nd}$  variation rate was  $\sim 150\%/Oe$  which is about 15 times larger than that of  $V_{1st}$ . The detection of the second harmonic voltage offers the potential for a great improvement in the magnetic field sensitivity.

KEYWORDS: second harmonic, magnetic sensor, impedance, amorphous ribbon

Magneto-resistance (MR) sensors have been developed for high density magnetic recording and various sensing systems. Since the giant magneto-resistance (GMR) effect was discovered in superlattice films<sup>1,2)</sup> in 1988, it has been studied for application to high density magnetic recording heads. A practical GMR sensor has not yet been realized because it requires a strong magnetic field and exhibits a large hysteresis.

Recently, the magneto-impedance (MI) effect<sup>3-5)</sup> has been investigated as regards applications to highly sensitive magnetic sensors. The MI effect is based on the impedance change in a magnetic wire or a thin film which occurs when a radio frequency (RF) current is passed through it and an external magnetic field ( $H_{ex}$ ) is applied. One of the authors also reported a magnetic (M)/conductor (C)/magnetic (M) film sensor through which the RF current passes and whose impedance changes with  $H_{ex}$ .<sup>6-8)</sup> A high-speed and highly sensitive magnetic sensor was achieved by employing NiFe/SiO<sub>2</sub> multilayer patterned film as the magnetic film and operating it at a high frequency of several hundred MHz. In these impedance-changing type sensors, the impedance change is detected as a voltage change at a fundamental frequency.

Another approach has been the development of the fluxgate sensor which is also a highly sensitive magnetic sensor.<sup>9)</sup> A fluxgate sensor is generally composed of a magnetic core surrounded by two wound coils. An AC input current is supplied to one coil and an output voltage is detected from the other. The output voltage contains a second harmonic component at  $H_{ex} \neq 0$  Oe and contains no second harmonic component at  $H_{ex} = 0$  Oe. This second harmonic component is proportional to  $H_{ex}$  and is used as a sensitive measure of  $H_{ex}$ . Since the second harmonic component is attributed to an asymmetric hysteresis loop of the core when  $H_{ex}$  is applied, a similar phenomenon can be expected in the impedance-changing type sensors. In this paper, we investigate the features of second harmonic generation in an M/C/M sensor with the view to further improving its sensitivity.

Figure 1 is a schematic diagram of the M/C/M sensor. The sensor is composed of a Cu wire with two current ( $I_1, I_2$ ) and two voltage ( $V_1, V_2$ ) electrodes and of Co<sub>68.5</sub>(Fe, Mn, Mo)<sub>7.5</sub>(Si, B)<sub>24</sub> amorphous ribbons which sandwich the wire from above and below on a glass substrate. The dimensions are  $l_m = 10$  mm,  $w_m = 10$  mm,  $t_m = 10$  mm and  $d_c = 0.2$  mm. The ribbon exhibited a saturation magnetization ( $4\pi M_s$ ) of 6 kG, an electric resistivity ( $\rho_m$ ) of  $120 \mu\Omega\cdot\text{cm}$ , a saturation magnetostriction ( $\lambda_s$ ) of

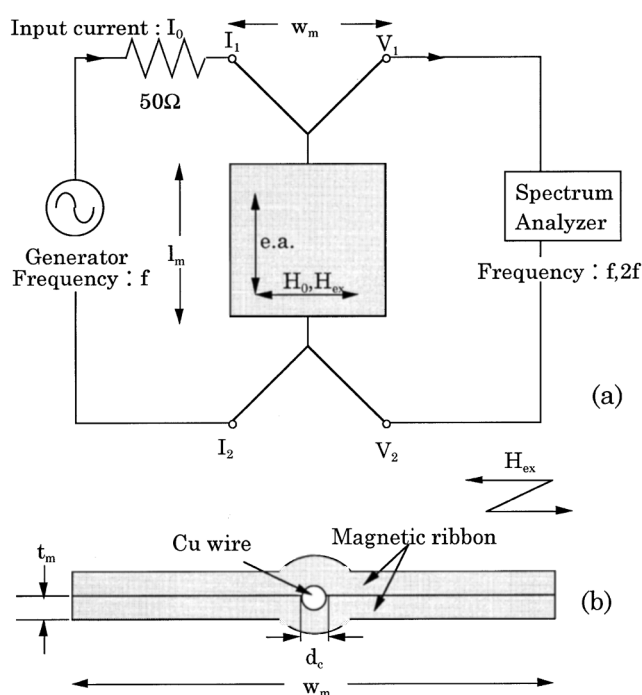


Fig. 1. Schematic diagram of the M/C/M sensor and measurement setup. (a) in-plane, (b) cross-section.

$\sim 0$  and a uniaxial anisotropy magnetic field ( $H_k$ ) of  $\sim 4.8$  Oe. The easy axis of the ribbons was in the  $l_m$  direction, and  $H_{ex}$  ( $\pm 60$  Oe) was applied in the  $w_m$  direction with a permanent magnet. An RF current ( $I_0$ ) of 15 mA was supplied to electrodes  $I_1$  and  $I_2$  with a generator (Kenwood, AG-203D), thus causing a driving field ( $H_0$ ) in the amorphous ribbons. The output signal from electrodes  $V_1$  and  $V_2$  was measured with a spectrum analyzer (HP, 4195A). The RF current frequency was 500 kHz. A  $50 \Omega$ -resistance was connected between the generator and the sensor to match the impedance.

First, we consider the second harmonic generation mechanism in the M/C/M sensor. Figure 2 shows the observed (solid line) and idealized (dashed line) hysteresis loops for an amorphous ribbon. The ribbon and the sensor had the same shape. Measuring field was applied in the direction of the hard axis. In Fig. 2, the driving field ( $H_0$ ) magnetization flux density ( $B$ ) and output voltage ( $V$ ) are also shown.  $H_0$  is assumed to be applied to the idealized hysteresis loop. The total impedance ( $Z_t$ ) of a practical sensor is described as follows;

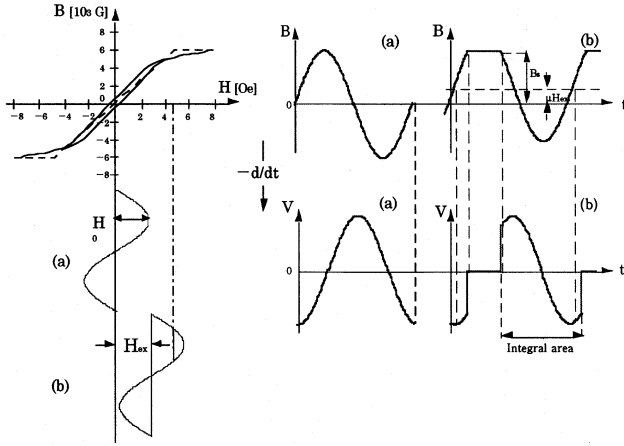


Fig. 2. Observed (solid line) and idealized (dashed line) hysteresis loops, and the second harmonic generation mechanism. (a)  $H_{ex} = 0$  Oe, (b)  $H_{ex} \neq 0$  Oe.

$$Z_t = Z_c + Z_m, \quad (1)$$

where  $Z_c$  is the impedance due only to the Cu wire.  $Z_m$  is the impedance related to the permeability of the ribbon and changes greatly when  $H_{ex}$  is applied. In order to simplify the  $V_{2nd}$  generation mechanism, we considered that  $Z_t$  is composed only of  $Z_m$ . In Figs. 2(a) and 2(b),  $H_{ex} = 0$  and  $H_{ex} \neq 0$  Oe, respectively. The relation between  $V$  and  $B$  is presented as follows;

$$V = -d\Phi/dt, \quad (2)$$

where  $\Phi$  is magnetic flux and

$$\Phi = SB = LI_0, \quad (3)$$

where  $S$  is the total section area of the ribbons, and  $L$  is the inductance due to the ribbons. The above equations indicate that the variation in  $B$  is equivalent to that in  $L$ .  $L$  is proportional to  $Z_m$ . When  $H_{ex} = 0$  Oe, the ribbon is magnetized symmetrically every half cycle of  $H_0$  and this results in the symmetric variations in  $B$  and  $V$  as shown in Fig. 2(a). The Fourier expansion of  $V$  has only odd terms. When  $H_{ex}$  is sufficiently large such that  $H_0 + H_{ex}$  exceeds  $H_k$ , as shown in Fig. 2(b),  $B$  is partially saturated which is the reason for difference between the positive and negative amplitudes of  $B$ . Consequently, the Fourier expansion of  $V$  contains even terms. The first and second terms of the Fourier expansion are respectively the amplitudes of  $V$  at the fundamental frequency ( $V_{1st}$ ) and the second harmonic frequency ( $V_{2nd}$ ).

Figure 3 shows the equivalent circuit of the sensor. When  $I_0$  is supplied to  $I_1$  and  $I_2$   $H_0$  of about 1.3 Oe is reflected and/or absorbed in the ribbons, and  $Z_m$  is then generated.<sup>8,9)</sup> An increase of the impedance change requires a higher  $Z_m$  and lower  $Z_c$ .  $Z_t$  at 500 kHz was measured with a network analyzer (HP, 85047A). The  $Z_t$  values at  $H_{ex} = 0$  and  $H_{ex} = 500$  Oe were 650 and 310 m $\Omega$ , respectively. From this result  $Z_m$  was calculated to be 340 m $\Omega$  which is almost the same as  $Z_c$ .

Then, we calculate the voltage at the fundamental frequency ( $V_{1st}$ ) and that at the second harmonic frequency ( $V_{2nd}$ ). Figure 4 shows the  $H_{ex}$  dependences of  $V_{1st}$  and  $V_{2nd}$  represented in dBm.  $H_0$  is assumed to be  $H_k/2$ .  $V_{1st}$  and

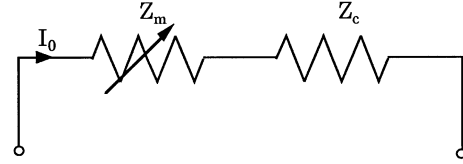


Fig. 3. Equivalent circuit of the M/C/M sensor.

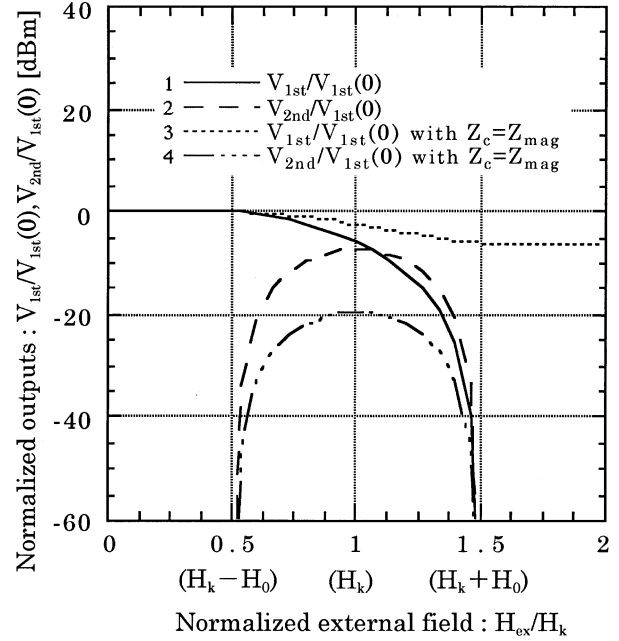


Fig. 4. Relation between the external field and the calculated outputs at the fundamental and second harmonic frequencies.

$V_{2nd}$  are normalized by  $V_{1st}$  at  $H_{ex} = 0$  Oe ( $V_{1st}(0)$ ) and  $H_{ex}$  is normalized by  $H_k$ . Lines 1 and 2 show  $V_{1st}/V_{1st}(0)$  and  $V_{2nd}/V_{1st}(0)$  at  $Z_c = 0 \Omega$ , respectively. Lines 3 and 4 show  $V_{1st}/V_{1st}(0)$  and  $V_{2nd}/V_{1st}(0)$  at  $Z_c = Z_m$ , respectively. As  $H_{ex}$  is increased  $V_{1st}/V_{1st}(0)$  at  $Z_c = 0 \Omega$  (line 1) begins to drop at  $H_k - H_0$  and disappears at  $H_k + H_0$ . The rate of decrease of  $V_{1st}$  is then maximum at  $H_{ex} = H_k + H_0$ . By contrast,  $V_{2nd}/V_{1st}(0)$  at  $Z_c = 0 \Omega$  (line 2) appears at  $H_{ex} = H_k - H_0$ , reaches its maximum at  $H_{ex} = H_k$  and disappears at  $H_{ex} = H_k + H_0$ . The variation rate in  $V_{2nd}$  has its maximum at  $H_{ex} = H_k \pm H_0$ . When  $Z_c = Z_m$ ,  $V_{1st}/V_{1st}(0)$  (line 3) begins to decrease at  $H_{ex} = H_k - H_0$  and attains a certain value at  $H_{ex} \geq H_k + H_0$ . The maximum rate of decrease in  $V_{1st}$  which is obtained at  $H_{ex} = H_k$  is smaller than that at  $Z_c = 0 \Omega$ . On the other hand  $V_{2nd}/V_{1st}(0)$  at  $Z_c = Z_m$  (line 4) shows a similar variation to that at  $Z_c = 0 \Omega$  (line 2); the variation rate in  $V_{2nd}$  is maximum at  $H_{ex} = H_k \pm H_0$ . Consequently, it is estimated that the variation rate in  $V_{2nd}$  is larger than that in  $V_{1st}$  in a practical case such as  $Z_c = Z_m$ .

Experimental results are shown in Fig. 5. The variations in  $V_{1st}$  and  $V_{2nd}$  show the same tendencies as the theoretical ones (lines 3 and 4 in Fig. 4). Neither hysteresis nor a Barkhausen jump are detected. The variation rate in  $V_{1st}$  ( $VR_{1st}$ ) and that in  $V_{2nd}$  ( $VR_{2nd}$ ) are defined as follows.

$$VR_{1st} = 10^{[(V_{1st}(H+1) - V_{1st}(H))/20]} \% / \text{Oe}, \quad (4)$$

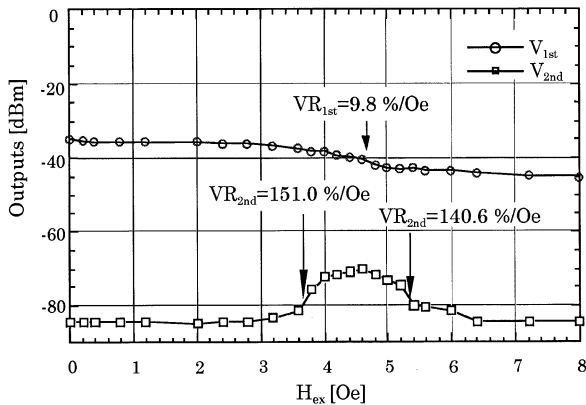


Fig. 5. External field ( $H_{ex}$ ) dependence of the outputs at the fundamental and second harmonic frequencies.

$$VR_{2nd} = 10^{\{[V_{2nd}(H+l) - V_{2nd}(H)]/20\}} \% / \text{Oe}. \quad (5)$$

where  $V_{1st}(H)$  and  $V_{2nd}(H)$  are respectively the  $V_{1st}$  and  $V_{2nd}$  values when  $H_{ex} = H$  Oe.  $VR_{1st}$  reaches its maximum (9.8%/Oe) at  $H_{ex} = 4.8$  Oe ( $\equiv H_k$ ).  $VR_{2nd}$  has its maximum values of 140.6 and 151.0%/Oe at  $H_k = 3.6$  and 5.6 Oe ( $\equiv H_k \pm H_0$ ), respectively. The fact that the maximum  $VR_{2nd}$  value is about 15 times larger than that of  $VR_{1st}$  illustrates the great advantage of detecting  $V_{2nd}$  in terms of developing a highly sensitive magnetic sensor.

In summary, we investigated, theoretically and experimentally, the second harmonic generation mechanism in an impedance-changing type sensor which was composed of a Cu wire sandwiched between Co-based amorphous ribbons.

The variations in output voltage, which are proportional to the impedance, at the fundamental and second harmonic frequencies were in good agreement with the calculated values. We obtained a maximum voltage variation rate of 9.8%/Oe at the fundamental frequency and of 151.0%/Oe at second harmonic frequency. This large voltage variation rate in the second harmonic is promising as regards successfully developing a higher sensitivity than the previously reported impedance-changing type sensors, in which a voltage change at the fundamental frequency is detected.

#### Acknowledgment

The authors thank Dr. Masakatsu Senda at NTT Laboratories and Mr. Kazumasa Makita at Yamagata University for their useful discussions. The authors would like to thank Mr. Shunsuke Arakawa of Hitachi Metals, Ltd. for supplying Co-based Amorphous ribbons.

- 1) M. N. Baibich, J. M. Broto, A. Fert, F. Nguyen, V. Dau, F. Petroff, P. Etienne, G. Creuzet, A. Friedrich and J. Chazelas: Phys. Rev. **61** (1988) 2472.
- 2) T. Sinjo and H. Yamamoto: J. Phys. Soc. Jpn. **59** (1990) 3061.
- 3) K. Mohri, T. Kohzawa, K. Kawashima, H. Yoshida and L. V. Panina: IEEE Trans. Magn. **28** (1992) 3150.
- 4) L. V. Panina and K. Mohri: J. Magn. Soc. Jpn. **18** (1994) 245.
- 5) K. Bushida, M. Noda, L. V. Panina, H. Yoshida, T. Uchiyama and K. Mohri: J. Magn. Soc. Jpn. **18** (1994) 493.
- 6) M. Senda, O. Ishii, Y. Koshimoto and T. Toshima: IEEE Trans. Magn. **30** (1994) 4611.
- 7) M. Senda, O. Ishii, Y. Koshimoto and T. Toshima: J. Magn. Soc. Jpn. **19** (1995) 465.
- 8) M. Senda, K. Takei, O. Ishii and Y. Koshimoto: IEEE Trans. Magn. **32** (1996) 3485.
- 9) D. I. Gordon and R. B. Brown: IEEE Trans. Magn. **MAG-8** (1972) 76.